**ORIGINAL ARTICLE**

# A new methodology to establish the relationship between equivalent shot velocity and air pressure by surface roughness for shot peening

Chengyu Wang[1] · Weigang Li[1] · Jianjun Jiang[2] · Xin Chao[2] · Weikui Zeng[2] · Jie Yang[1]

**Abstract**

The study of shot peening process by numerical simulation is becoming mature and efficient. Shot velocity is very important, which is related to the accuracy of simulation results. However, the actual shot peening process was directly controlled by air pressure and other parameters, instead of shot velocity. This paper details a new method to obtain the equivalent shot velocity as initial velocity used in simulation corresponding to air pressure in the actual shot peening. Firstly, under the same shot peening parameters, the linear relationship between the roughness and air pressure, and the linear relationship between the roughness and equivalent shot velocity were obtained by experiment and simulation, respectively. Secondly, the relationship between equivalent shot velocity and air pressure is established by the intermediate surface roughness. At last, the validity and reliability of the relationship be verified by arc height, residual stresses, coverage, and existing literature. In addition, this paper introduces a new method to calculate the number of shots used in combined discrete element model (DEM) and finite element model (FEM), taking into account the mass flow, nozzle movement speed and nozzle-workpiece distance, and other parameters. In this way, it is of significance to characterize the shot peening equipment rapidly and obtain the equivalent shot velocity used in the simulation to optimize the shot peening parameters in the aerospace and automotive industry.

## 1 Introduction

Shot peening (SP) is a mature forming method that improves the wear resistance and fatigue life of parts, especially, aircraft skin panels. A large number of shots repeatedly hit the metal surface, causing plastic deformation of the surface layer. The surface layer material extrudes each other and tends to be extended. The remaining material resists the extension of the surface layer. Therefore, the surface layer produces compressive stress and the rest of the material produces tensile stress. The shot peening process is also frequently used in the shape forming of sheet components to produce a desired curvature and shape or to correct the shape of a component, especially for forming contoured integral aircraft skin panels.

✉ Jie Yang
 yangchenjie@swjtu.edu.cn

1 School of Mechanics and Engineering, Southwest Jiaotong University, Chengdu 610031, Sichuan, People's Republic of China

2 Engineering Department, Chengdu Aircraft Industry (Group) Co. LTD, Chengdu 610091, Sichuan, People's Republic of China

In the actual shot peening process, the Almen intensity is a simple and rapid standard method for evaluating shot peening effects, and was controlled by air pressure and other parameters instead of shot velocity. Many researchers have performed studies on the Almen intensity and parameter optimization by the experimental method. For instance, Miao et al. [1] experimentally related the saturation and surface coverage of aluminum Al2024 to the peening time under different air pressure. Hu et al. [2] reported using experimental methods that an increase in the applied Almen intensity results in enhancing the resulting arc height. Experimental method can study the effect of shot peening under different air pressure, coverage, and shot size. It is difficult to study the change in the process.

Numerical tools and theoretical approaches have been widely used to study the Almen intensity in shot peening. For example, Jebahi et al. [3] have further developed the coupling model of discrete elements and finite elements (DEM-FEM) in ABAQUS, and proposed a 3D random DEM-FEM coupling model to simulate arc height of the Almen strip under different shot velocity. The simulation results by the DEM-FEM coupling model are in good agreement with the experimental results. Miao et al. [4] and Zhang et al. [5]

proposed analytic models for predicting the Almen intensity. These analytical models relate the arc height to shot velocity and other parameters.

In a word, the experimental method is mainly to study the influence of different air pressure and other parameters on the Almen intensity with the shot peening machine, while the simulation and theoretical analysis method is mainly to study the influence of known shot velocity and other parameters on the Almen intensity as shown in Fig. 1. It is inevitable to establish the relationship between shot velocity and air pressure through simulation and theoretical methods guide actual production and optimization.

In the past few decades, the relationship between the shot velocity and air pressure is seldom reported for a shot peening process. Due to differences in the type and performance of shot peening machines, the experiments showed that the relationship between the shot velocity and the air pressure, summarized by Klemenz et al. [6] through semi-experiential formula is not applicable to all peening machines unfortunately. For example, compressed air machines, the velocity of the shot flow at a certain time was measured usually by specialized measurement device. Bill et al. [7] reported that a kind of shot velocity measurement device, called ShotMeter, can be used to determine the velocity of a few shots rather than all the shots involved in the operation. However, it is reported by Mylonas et al. [8] that the shot velocity from the nozzle to the metal surface is not constant and the impact velocity is also likely to vary from one shot to another. Gariépy et al. [9] presented that only 20% of the shots are expected to impact the treated surface at their initial velocity. The detailed distribution of impact velocities at the treated surface was reported

by Tu et al. [10] and Hong et al. [11]. In fact, the present method is also taken to measure the real velocity of several shots as the initial velocity of all shots used in the simulation. Nordin et al. [12] proposed an experimental method to predict the shot velocity by comparing indentations on a test plate. This method is more suitable for small shot and is limited to a single small size shot for a low coverage. Liu et al. [13] proposed a new kinematic model of shots that was used to predict shot velocity. Miao et al. [14] reported that needle velocity was experimentally calibrated using high-speed camera. It is concluded that there are few researches and the current method is not universal due to the difference of machines.

In fact, as Jebahi et al. [3] mentioned that we only need the equivalent shot velocity which each shot has the same initial velocity be used in numerical simulation, instead of each shot real velocity corresponding to the air pressure (see Fig.1), (it is impractical to measure the real velocity of all the shots involved), and the Almen intensity, residual stress and surface roughness should be consistent with the experiment result under same SP parameters. As the characterization of the surface morphology after shot peening, the surface roughness is easier and faster to measure, meanwhile, it is one of the important indexes to evaluate the shot peening effect. Previous literature suggests that the surface roughness obtained by the simulation method is consistent with that obtained by experimental method. Bagherifard et al. [15] and Liu et al. [16] reported that the surface roughness stabilizes when the coverage increases to 100%. It is reported by Taro et al. [17] that there are 3 stages in surface roughness evolution when the polished surface is during shot peening process. The roughness value increases rapidly in the first stage. The surface
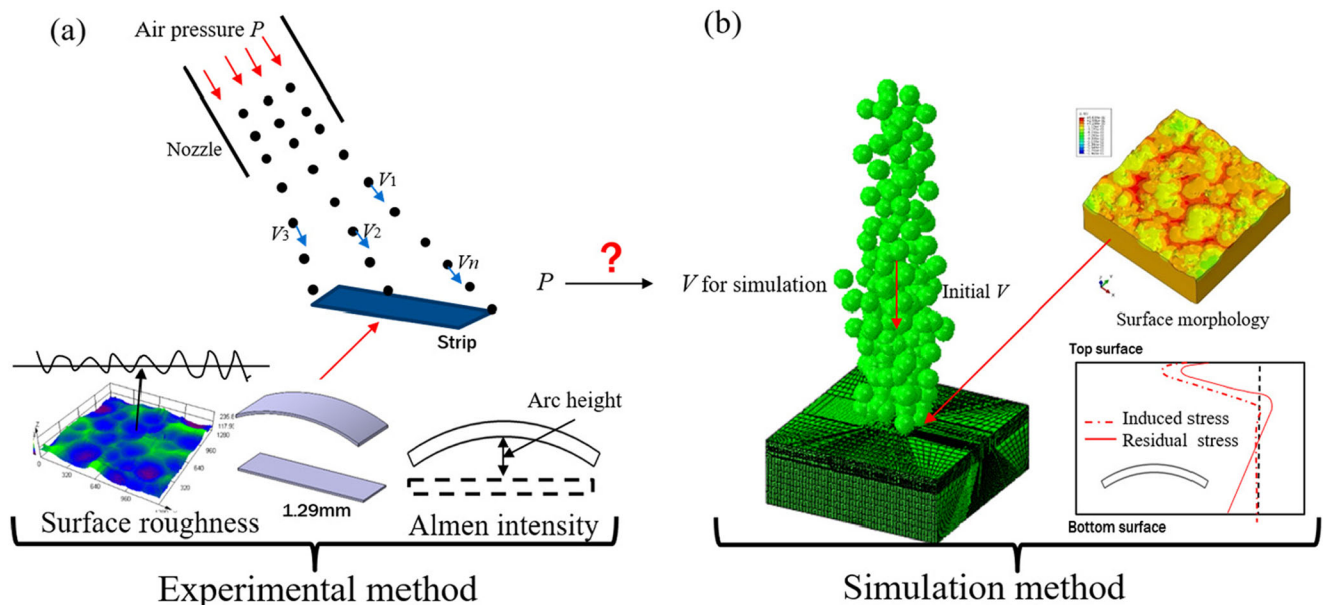


**Fig. 1** Shot velocity $V$ for simulation is determined by air pressure $P$. (**a**) The experimental method is mainly to obtain surface roughness, arc height, and Almen intensity by air pressure. (**b**) The simulation method is mainly to study surface roughness, residual stress, arc height, and Almen intensity by shot velocity instead of air pressure

indents are becoming smoother in the second stage. Finally, in the third stage, the surface roughness no longer changes greatly. Meanwhile, Lin et al. [18] studied the surface coverage, roughness, and residual stress after shot peening by FEM. It finds that the surface roughness increases with the shot velocity. Miao et al. [1] demonstrated that the surface roughness increases with air pressure by the experimental method. Chen et al. [19] and Taro et al. [17] concluded the surface roughness increases with the increase of the shot velocity, and the surface roughness has an approximate linear relationship with the shot velocity. Liu et al. [16] and Kumar et al. [20] explored that the surface roughness increases with the increase of the air pressure, and the surface roughness has an approximate linear relationship with the air pressure. The roughness parameters obtained from numerical simulation correspond quite well with the roughness values measured experimentally. However, most of the surface roughness numerical studies in the literature have not considered mass flow, nozzle movement speed and nozzle-workpiece distance and other parameters, and the shot-shot interaction in actual shot peening.

The purpose of this study is to determine equivalent shot velocity for simulation corresponding to the air pressure in the actual shot peening process. The primary difference between this work and the work reported in the available literature is that it induces a new methodology to establish the relationship between air pressure and equivalent shot velocity through intermediate surface roughness for characterizing the shot peening equipment. Meanwhile, this paper introduces a new method to calculate the number of shots used in DEM-FEM, considering mass flow, nozzle movement speed and nozzle-workpiece distance, and other parameters, in actual shot peening. The advantage of the new method is that the simple linear relationship between air pressure and equivalent shot velocity is efficient and reliable to avoid measuring real shot velocity by high-speed cameras, and ensures the natural match between simulation results and experimental results. And, the DEM-FEM model proposed in this paper is convenient and

fast with a smaller amount of computing time and considering the interaction between shots is closer to the real shot peening situation. By this new method, the equivalent shot velocity can be determined quickly and then the actual production and optimization can be guided by simulation analysis and theoretical analysis.

In Section 2.1, we describe the new method of establishing the relationship between air pressure and equivalent shot velocity. In Section 2.2, surface roughness under different air pressure conditions is obtained by experiment method for the Almen-like strips (alloy aluminum 7075-T651). In Section 2.3, it introduces DEM-FEM coupling model to predict the effects of the shot peening process, including collisions between shots. In Section 2.3.4, a new method for calculating the number of shots taking into account the mass flow and other parameters is proposed. The relationship between air pressure and equivalent shot velocity is demonstrated in Section 3. We have characterized the shot peening equipment with an aim to relate the equivalent shot velocities to the tool's air pressure. The obtained equivalent shot velocity was input as initial velocity in a coupling DEM-FEM for real Almen-sized alloy aluminum 7075-T651 strips. The predicted residual stresses, arc heights, and coverage were verified and discussed in Section 4. Finally, conclusions are presented in Section 5.

## 2 The relationship between air pressure and shot velocity

### 2.1 A general introduction to the new method

There are two ways to get surface roughness by experimental method and simulation as shown in Fig. 2. At first, the relationship between surface roughness and air pressure was obtained by shot peening machine and roughness measuring equipment. Surface roughness has an approximate linear

**Fig. 2** A new method for establishing the relationship between $P$ and $V$
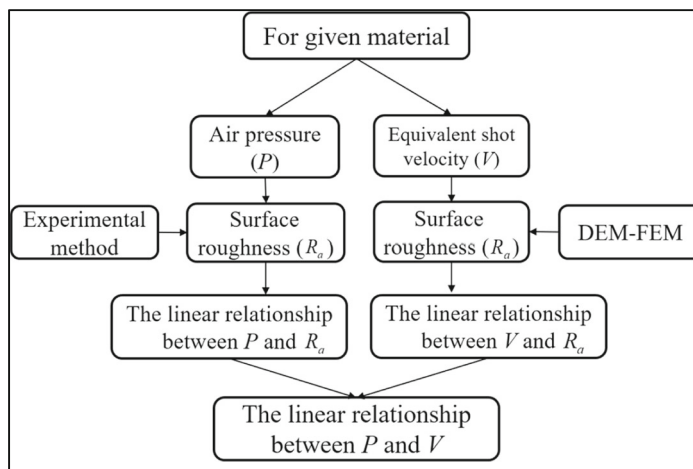
relationship with air pressure, which is shown below in Eq. (1). Secondly, the relationship between surface roughness and equivalent shot velocity was obtained by simulation under the same shot peening parameters as the experimental conditions. Surface roughness has an approximate linear relationship with the shot velocity, which is shown below in Eq. (2). Thirdly, the relationship between shot velocity and air pressure is established through the intermediate surface roughness, as shown below in Eq. (3). At last, equivalent shot velocity $V$ has an approximate linear relationship with air pressure $P$, which is shown below in Eq. (4).

$$R_a = f(P) = a_1 P + b_1 \tag{1}$$

$$R_a = f(V) = a_2 V + b_2 \tag{2}$$

$$R_a = a_1 P + b_1 = a_2 V + b_2 \tag{3}$$

$$V = \frac{a_1}{a_2} P + \frac{(b_1 - b_2)}{a_2} = aP + b \tag{4}$$

where $a$ is equal to $a_1$ over $a_2$, $b$ is equal to $(b_1 - b_2)$ over $a_2$.

## 2.2 Experiments

### 2.2.1 Equipment and experimental methods

Shot peening process is accomplished with high precision mobile blasting machine, combined with SIMENS industrial robot with 840D robot controller. Figure 3(a) shows the blasting machine. The strips are fixed at the Almen holder as shown in Fig.3b. During shot peening process, the moving velocity of the nozzle is 1000.0 mm/min and mass flow is 5.0 kg/min or 6.0 kg/min. S230 steel shots with the diameter of 0.58 mm is used in all experiment as shown in Fig. 4a. Shot peening experiments is applied on the target material, Al 7075-T651.

Almen-sized Al 7075 strips are cut from 78-mm thick alloy aluminum 7075-T651 sheets by wire electrical discharge machining. The test strip with dimensions 76.0 mm × 19.0 mm × 1.29 mm is same size as the Almen strip of the type A (SAE 1070 spring steel) as shown in Fig. 4b. For given shot type, mass flow, and other process parameters, the operation parameters were selected for air pressure, $P$, as 1.0, 1.5, 2.0, 2.5, and 3.0 bar. In order to evaluate coverage, visual inspection is used as a standard method in actual shot peening. For practical purposes, 98% coverage is usually considered as 100% coverage. For the given shot-type 230, mass flow 5 kg/min and other process parameters, coverage has exceeded 100% when air pressure is over 1.0 bar.

### 2.2.2 Surface roughness obtained by experimental method

The average surface roughness $R_a$ at different air pressure was obtained by Olympus OLS4100 CLSM. The surface roughness is measured using a 12-mm evaluation length, while the 3D topography is displayed at × 10 magnification. The measured area is 224 mm$^2$ and the detecting instrument accuracy was in (0.12–0.01) μm. For the shot-type S230, the measured area has hundreds of indents, enough to represent the entire shot peening surface. Each strip was detected 3 times, and the average $R_a$ was taken. Figure 5a displays the 2D morphology of the surface layer and indentation of a sample section after shot peening can be observed by an optical microscope. Figure 5b presents the 2D surface topography of a sample section.

## 2.3 DEM-FE coupling model

It is a method to simulate the shot peening process and obtain surface roughness under different shot velocity. The first is to
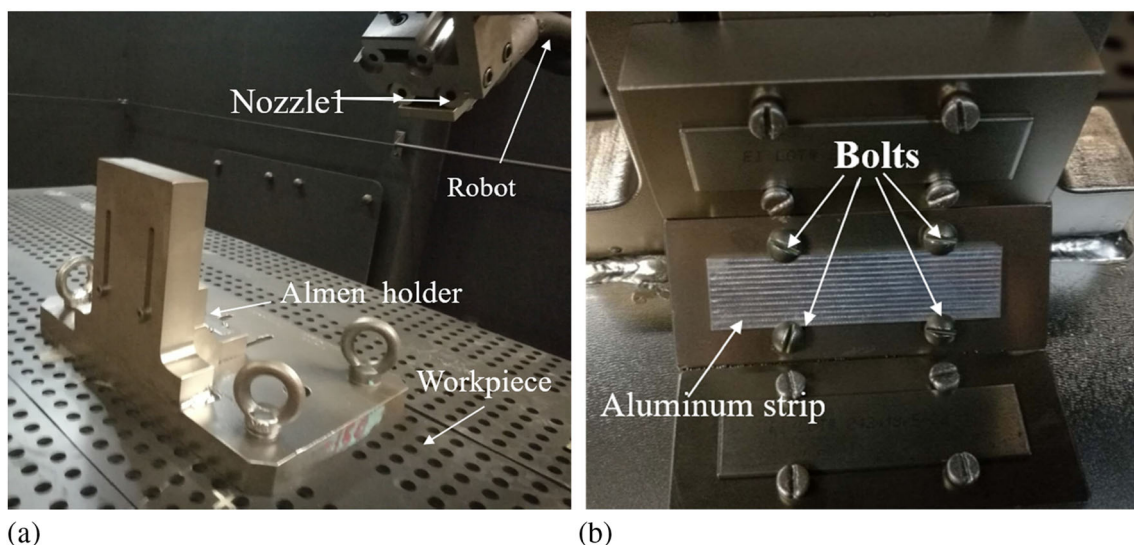


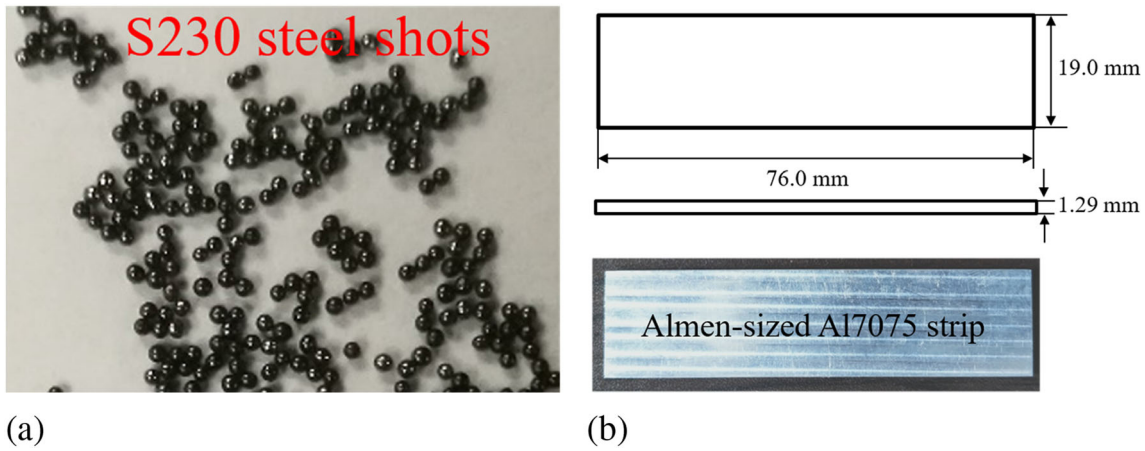**Fig. 3** **a** Shot peening equipment. **b** Almen holder

Fig. 4 **a** S230 steel shots. **b** Almen-sized Al7075-T651 strip

determine the number of shots at least 100% coverage, taking into account the mass flow rate and other parameters, and the second is to take the collision between shots into account. One of the most common roughness parameters used in the field of shot peening is $R_a$. The surface roughness under different shot velocity and mass flow can be calculated by the displacement statistics of the node in the measuring area.

### 2.3.1 DEM-FEM

It is reported by Wang et al. [21] and Gangaraj et al. [22] that representative elementary volumes (REVs) are an effective simulation method for shot peening. In order to be consistent with the test area of surface roughness, region 1 is of dimensions 3.0 mm × 3.0 mm; region 3 is of dimensions 2.08 mm × 2.08 mm. A volume of region 2, with dimensions 1.5 mm × 1.5 mm × 0.5 mm, is selected as a representative volume to study surface roughness and residual stress in Fig. 6a. The finite element mesh is comprised of 3D 8-node reduced integration elements. During the shot peening process, numerous shots impact the component surface at random locations. In order to simulate these randomly distributed shots, a random-shots PD3D element model is generated by using a Python program combined with Abaqus/Explicit as shown in Fig. 6b. Han et al. [23] reported that the mesh size of the region which produces large plastic deformation should be smaller than 1/10 of the shot diameter. Thereby, the mesh of the region which directly contacts with shots is refined, element size is 0.01 mm. The mesh size of region 3 was refined and the mesh size of the region far from the region 3 is relatively larger, and the total number of elements is 282,282 as shown in Fig. 6c. Figure 6d shows the entire 3D DEM-FEM random multiple-shot model, which takes into account the collision between the shots.
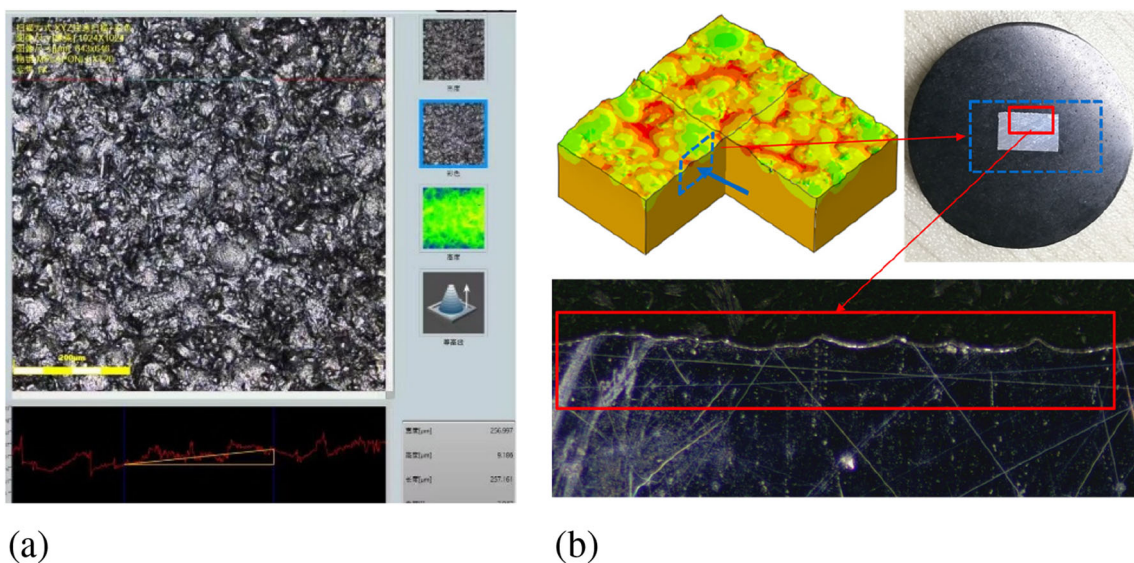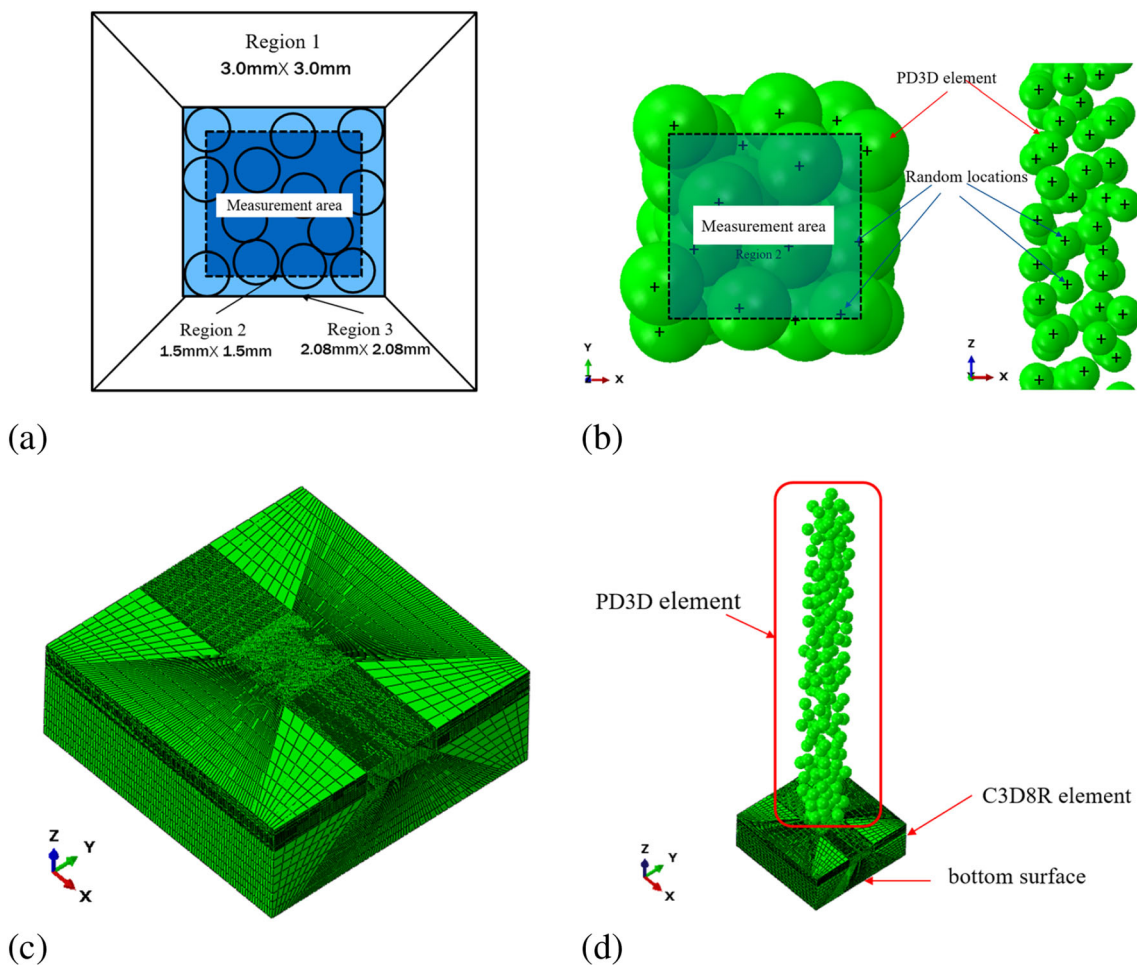


Fig. 5 Surface topography. **a** 2D surface topography of the surface layer. **b** 2D surface topography by optical microscope

**Fig. 6** **a** Representative surface (Region 1, fine element region; region 2, boundary of the shots centers; region 3, representative surface). **b** A random-shots PD3D element model. **c** Component mesh. **d** 3D DEM-FEM random multiple-shot model

There are four assumptions in this study: (1) All shots are rigid and have the same initial velocity. (2) Initial residual stress caused by machining and heat treatment is ignored in the DEM-FEM. (3) In the actual shot peening process, the bouncing shot will affect the shot that has not impact the metal surface yet, including changing the impact angle and reducing the shot velocity. Therefore, the collision between the shots is included in the DEM-FEM. (4) For the boundary condition, the material bottom surface is completely restrained $U_x = U_y = U_z = 0$.

### 2.3.2 Material model

Since very high strain rates are involved in the shot peening process, rate-dependent properties must be taken into account in the target component model. There are many well-verified mathematical models that consider strain rates in evaluating the stress-strain relations (Huang et al. [24]). Based on the work of Marini et al. [25], the isotropic hardening approach with rate-dependent properties correctly predicts the

mechanical response undergoing shot peening. Therefore, this approach is applied in this study. Here, the Johnson-Cook equation is employed to evaluate the stress-plastic strain relations:

$$\sigma = [A + B\varepsilon^n]\left[1 + C\ln\left(\dot{\varepsilon}^*\right)\right] \quad (5)$$

where $\sigma$ is the stress to be evaluated; $\varepsilon$ is the equivalent plastic strain; $\dot{\varepsilon}^* = \dot{\varepsilon}/\dot{\varepsilon}_0$ is the dimensionless strain rate for $\dot{\varepsilon}_0 = 1.0s^{-1}$, where $\dot{\varepsilon}_0$ is the reference values of strain rate

**Table 1** Mechanical property of the shot and alloy aluminum AL7075-T651

| Material | $\rho/(kg/m^3)$ | E/GPa | $\nu$ |
|---|---|---|---|
| Shot | 7800 | 210 | 0.3 |
| Al7075-T651 | 2810 | 71.7 | 0.3 |

**Table 2** Johnson-Cook material constants of alloy aluminum AL7075-T651 (Sheng et al. [26])

| Material | $A$ (MPa) | $B$ (MPa) | $C$ | $n$ |
|---|---|---|---|---|
| AL7075-T651 | 527 | 692 | 0.017 | 0.70 |

and $\dot{\varepsilon}$ are the strain rate; $A$, $B$, $C$, and $n$ are the four Johnson-Cook constants to be determined by a split Hopkinson bar experiment. In the current study, the effect of temperature increase due to peening is not included. In this work, the mechanical properties of the shot and Al7075-T651 are given in Table 1, and the Johnson-Cook constants are given by Sheng et al. [26] in Table 2. The Hertz mind in non-slip contact law has been utilized to model the shot-shot interaction and the shot-target surface interaction reported by Han et al. [27] and Murugaratnam et al. [28]. Regarding frictional behavior, Gariépy et al. [29] observed that differences in induced stresses were negligible for $0.1 < \mu < 0.5$. A friction coefficient of $\mu = 0.2$ was used in this work: the same value was reported by Miao et al. [30].

### 2.3.3 A new method for calculating numbers of shots, $N$

This paper introduces a new method to calculate the number of shots used in simulation, taking into account the mass flow, nozzle movement speed and nozzle-workpiece distance, and other parameters. At first, in the actual shot peening process, the work piece and the nozzle coordinate with each other to make the nozzle move relatively on the work piece surface according to the predetermined track. During the nozzle movement, shots impact on the surface of the part to form indentations. The indentations are distributed in a zonal pattern along the track of the nozzle, and normally distributed in the direction perpendicular to the track. To simplify the problem, we assume that the effective area of the indentations is a square, and that indentations in the square are distributed randomly and uniformly as shown in Fig.7a.

The simplified schematic diagram for calculating the number of effective shots impinged on the Almen strip is presented in Fig. 7b. $N_T$ is the number of total shots in the experiment. $N$ is the number of effective shots needed in the simulation. $t$ is the effective time for the shot impacting the strip with the nozzle moving at a speed of $V_R$, and the effective distance traveled is $l + h$. The definitions of $N_T$ and $N$ are presented in Eqs. (7) and (8), respectively.

$$t = \frac{(l + h)}{V_R} \tag{6}$$

$$N_T = \frac{Mt}{m_1} \tag{7}$$

$$N = \frac{A}{h(l + h)} N_T \tag{8}$$

where $m_1$ is the mass of a single shot, $l$ is the effective distance over which the shots impact the surface of the part, $h$ is the edge length of the effective shot peening area, $A$ is the area of representative surface, $V_R$ is the velocity of the nozzle, and $M$ is the mass flowrate.

### 2.3.4 100% coverage

The standard method of coverage evaluation is visual observation and statistics with magnifying equipment. According to the experiment, when the mass flow $M$ is 5.0 kg/min, velocity of the nozzle $V_R$ is (1000–1200) mm/min, and the air pressure is at the lowest 1.0 (bar); the coverage is 100% as shown in Fig. 8. In this paper, $h$ is equal to 70 mm according to the experiment. $l$ is equal to 76 mm and $V_R$ is equal to 1000 mm/min. $A$ is the area of representative surface. For shot-type S230, area of representative surface is equal to region 3, and approximately 1.3e5 shots randomly impact the alloy aluminum 7075-T651 strip surface with a surface size of 76.0 mm × 19.0 mm, equivalent to impact about 200 shots on region 2 (see Fig. 6) by using the formula 5. Therefore, $N$ is equal to 200 shot impacts for 100% coverage.
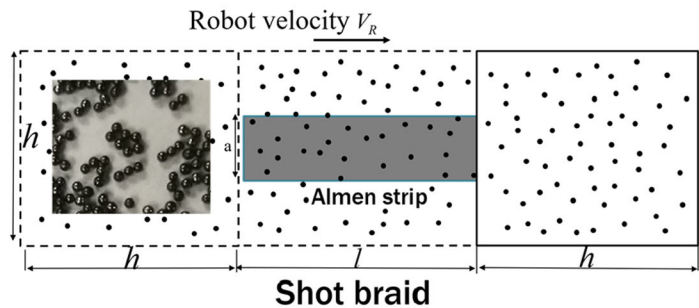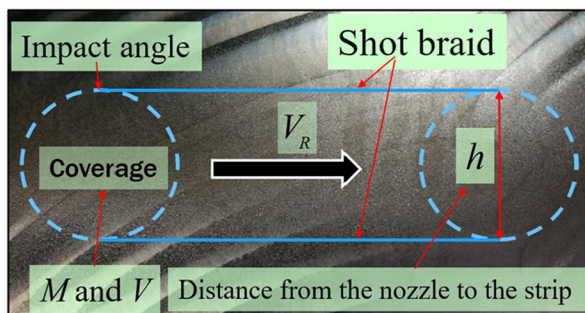


**Fig. 7** The proposed calculation method for the number of shots. **a** The effective square area on the strip. **b** Simplified schematic diagram
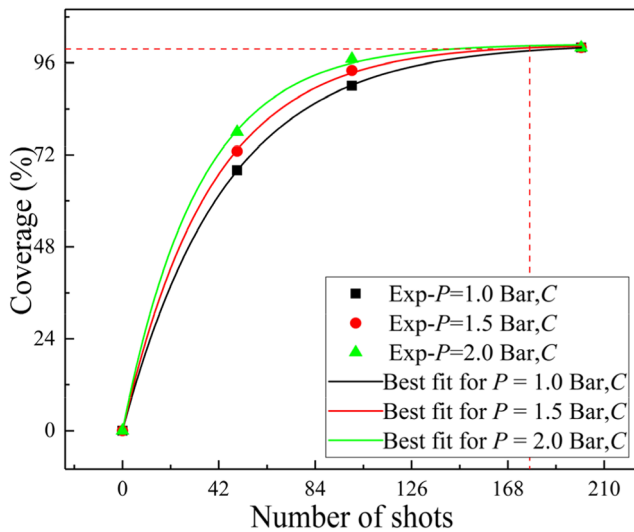
Fig. 8 100% coverage

### 2.3.5 Surface roughness obtained by simulation

Different shot velocities result in different surface roughness values. The parameter $R_a$ estimates the arithmetic mean deviation. Figure 9a presents the 3D morphology of the surface after shot peening in region 2. For the arithmetic average of the 3D roughness reported by Wu et al. [31], the experimental results validate the ability of the numerical model within the finite element framework in terms of the prediction of surface roughness as shown in Fig. 9b. It is expressed as:
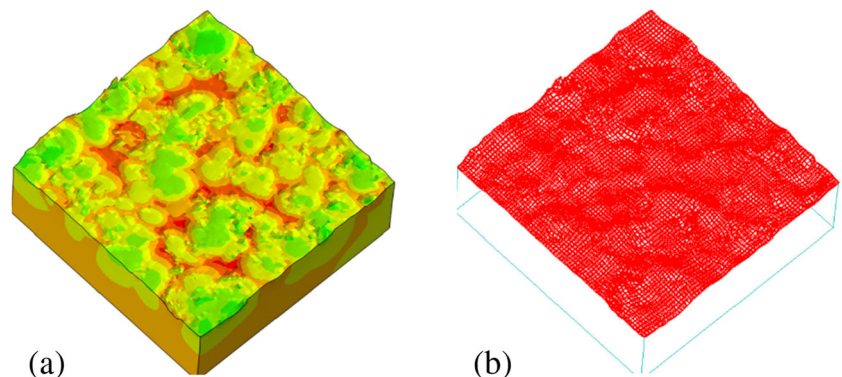
$$R_a = \frac{1}{n} \sum_i^n |U_i| \qquad (9)$$

where $U_i$ is the peening direction displacement, and $n$ is the number of all nodes on the measuring area.

## 3 Results

Under the same shot peening parameters, the linear relationship between average surface roughness and air pressure was

obtained by experimental method and the linear relationship between surface roughness and equivalent shot velocity was obtained by simulation. Then, the linear relationship between the equivalent shot velocity and the air pressure is established by the intermediate surface roughness.

### 3.1 Surface roughness measurements at different air pressure

The surface roughness $R_a$ value is 0.7 μm before shot peening and the surface topography is shown in Fig. 10a. After shot peening, the surface roughness of aluminum alloy increased significantly and Fig. 10b demonstrated 2D surface topography by optical microscope. Figure 11 shows the 3D surface topography and surface roughness $R_a$ values measured by the experimental method with different air pressure values.

Figure 12 shows the influence of shot peening process parameters on $R_a$ by the experimental method. $R_a$ increases significantly after shot peening process, compared to untreated samples ($R_a = 0.7$ μm). The results of the experiment show that the surface roughness has an approximate linear relationship with the air pressure and the error is 0.7 μm.

When the mass flow $M$ is 5 kg/min, the mathematical relationship between $R_a$ and air pressure $P$ ($P$ ranges from 1.0 to 3.0 bar) was established by regression equation, respectively

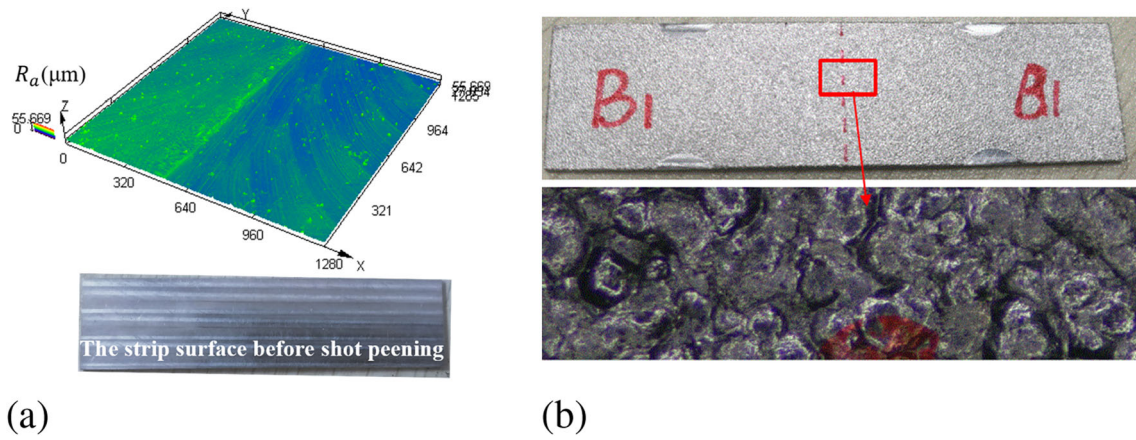$$R_a = f(P) = 3.2P + 2.0 \qquad (10)$$

where the goodness of fit is approximately 1.

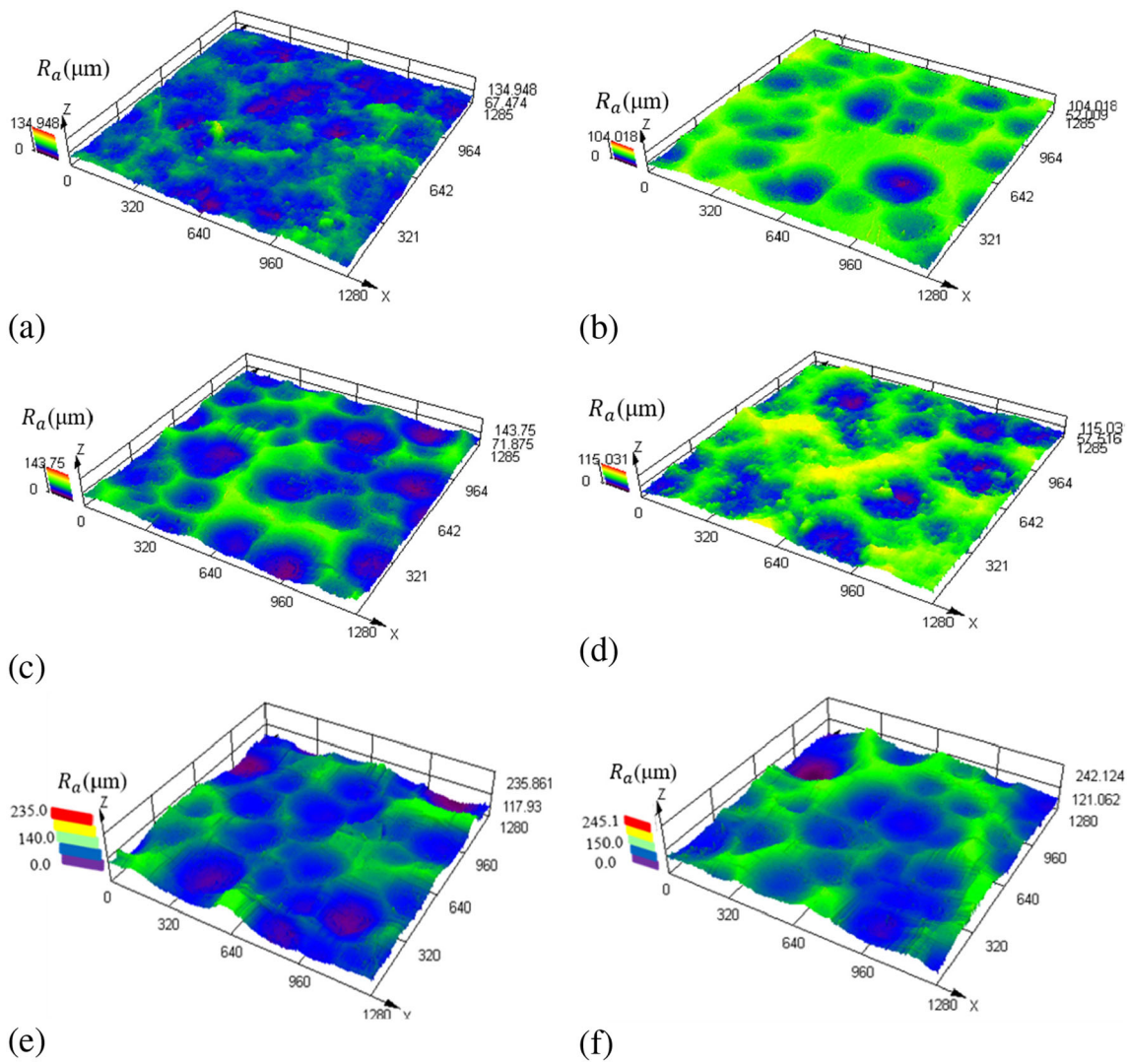### 3.2 Surface roughness studies at different shot velocity

The results of the numerical simulation show that the surface roughness increases as the shot velocity increases, as shown in Fig. 13.

Figure 13 shows that when the mass flow $M$ is 5 kg/min (shot number $N$ is 200), the trend exhibited by $R_a$ value is similar to which is reported by Bagherifard et al. [15]. Therefore, when, mass flow is 5.0 kg/min, the mathematical

Fig. 9 Roughness parameter $R_a$. a 3D morphology of the surface after shot peening. b All of the nodes on the measuring area after shot peening



(a)

(b)

(a)                                                    (b)

**Fig. 10** Roughness by experimental method. **a** Surface 3D morphology before shot peening. **b** Surface topography by optical microscope after shot peening



(a)                                                    (b)

(c)                                                    (d)

(e)                                                    (f)

**Fig. 11** Roughness by experimental method. **a** Air pressure equals 1.0 bar. **b** Air pressure equals 1.5 bar. **c** Air pressure equals 2.0 bar. **d** Air pressure equals 2.5 bar. **e** Air pressure equals 3.0 bar. **f** Air pressure equals 4.0 bar
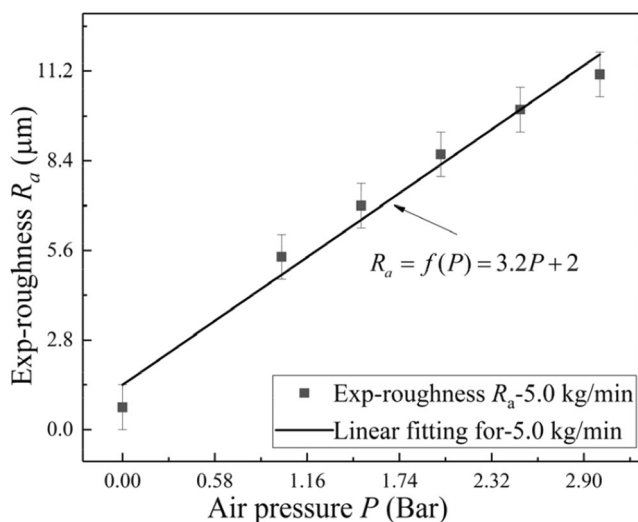
**Fig. 12** Linear fitting relationship between $R_a$ and $P$

relationship between $R_a$ and equivalent shot velocity $V$ ($V$ ranges from 30.0 m/s to 80.0 m/s.) was established by regression equation

$$R_a = f(V) = 0.24V - 2 \tag{11}$$

where the goodness of fit is approximately 1.

### 3.3 Relationship between air pressure and equivalent shot velocity

Previous literature suggests that increasing the coverage has little influence on the surface roughness, when the coverage is at least 100%. Therefore, we use the roughness as an intermediate variable to establish the relationship between equivalent shot velocity and air pressure, as shown in Fig. 14a. When mass flow is 5.0 kg/min, Fig. 14b shows that the mathematical
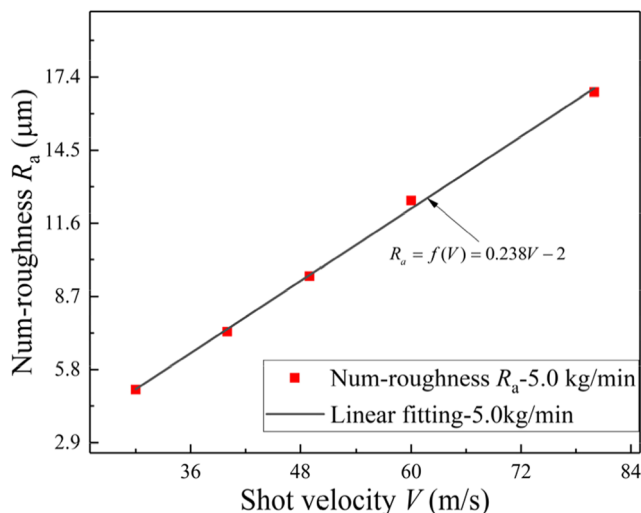


**Fig. 13** Linear fitting relationship between $R_a$ and $V$

linear relationship between equivalent shot velocity $V$ and air pressure $P$ was established by regression equation

$$V = f(P) = 13P + 18 \tag{12}$$

## 4 Discussion

### 4.1 Roughness parameter

A single roughness $R_a$ parameter may not be sufficient to describe the characteristics of surface topography and another commonly accepted surface roughness parameter is the root-mean-square deviation of three-dimensional surface roughness $R_q$. It is defined as:

$$R_q = \sqrt{\frac{1}{n} \sum_{i}^{n} U_i^2} \tag{13}$$

where $U_i$ represents the peening direction displacement, and $n$ represents the number of all nodes on the measuring area.

In order to study the symmetry and peakedness of the surface profiles, two other parameters, namely the skewness ($R_{sk}$) and the kurtosis ($R_{ku}$), have also been defined. The formula used to calculate the skewness of a profile are as follows:

$$R_{sk} = \frac{1}{nR_q^3} \left( \sum_{i=1}^{n} U_i^3 \right) \tag{14}$$

$$R_{ku} = \frac{1}{nR_q^4} \left( \sum_{i=1}^{n} U_i^4 \right) \tag{15}$$

Figure 15 shows the simulated surface roughness $R_a$ when the coverage rate was 100% for five different velocities: $v = 20$, 30, 40, 50, 60, and 70 m/s. This is clearly seen that surface roughness $R_{sk}$ unobviously increases with increasing shot velocity. With the increase of equivalent shot velocity, $R_{ku}$ first increases and then decreases. Surface roughness $R_a$ and $R_q$ increases gradually with increasing shot velocity. So far, $R_a$ is the most commonly used method to characterize the surface morphology. Meanwhile, the surface roughness under different air pressure is obtained experimentally, and it is easy to find the linear relationship between them. The similar result has been reported by [20] and Lin et al. [18]. Meanwhile, when the pressure is 1.0 bar, the roughness measured by the experimental method under different mass flow are very close, which may be because the low pressure cannot effectively push a large of shots out. Therefore in the actual shot peening, make sure the pressure is not too low. The surface roughness under different shot velocity is obtained by simulation, and it is easy to find the linear relationship between them. The similar result has been reported by Chen et al. [19] and Taro et al. [17]. Therefore, roughness $R_a$ and $R_q$ can be used as a suitable intermediate bridge to relate air pressure to equivalent shot velocity.
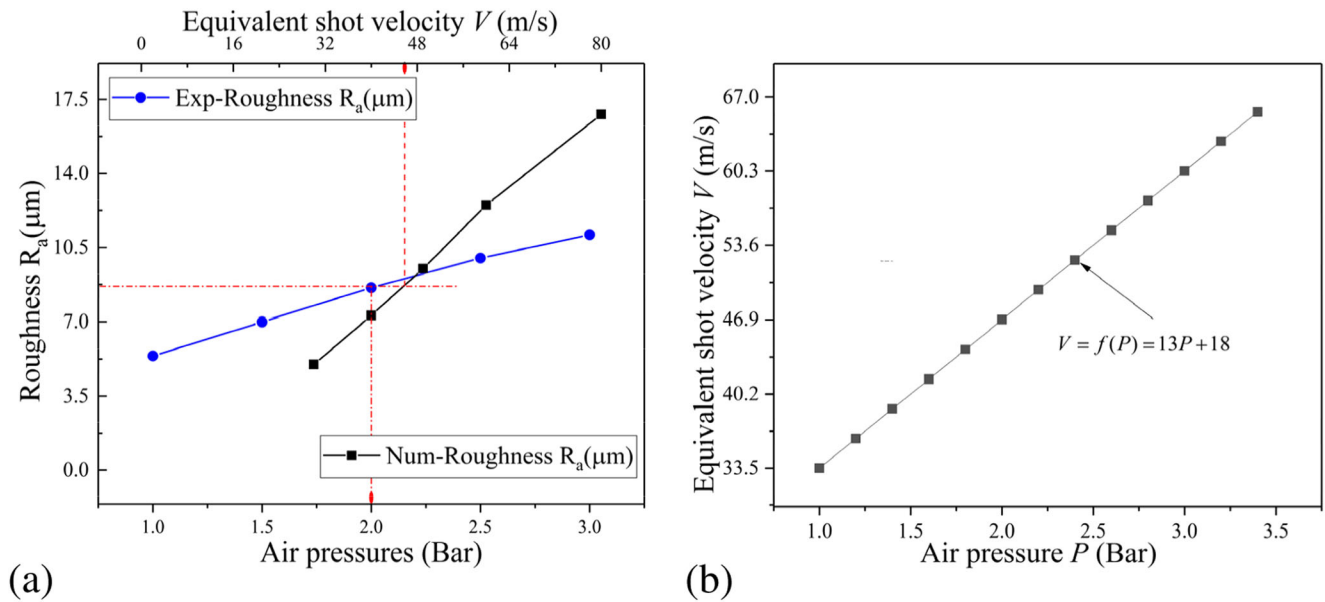
**Fig. 14** Relationship between air pressure and equivalent shot velocity. **a** Roughness as an intermediate variable. **b** Mathematical relationship between $V$ and $P$

## 4.2 Experimental verification

### 4.2.1 Arc height verification

We have characterized the shop peening equipment through the relationship between an aim to equivalent shot velocity and air pressure. The obtained equivalent shot velocities by the new method were input as initial velocity in a coupling DEM-FE model for real Almen-sized alloy aluminum 7075-T651 strips model. The predicted arc heights were finally compared against experimentally measured values. Arc height of alloy aluminum 7075-T651 strips was measured by Almen gauge, where air pressure $P$ is equal to 2.0, 2.5, 3.0 bar. Arc height of alloy aluminum 7075-T651 strips was directly

**Fig. 15** Surface roughness when coverage rate is 100% and velocities $v = 20, 30, 40, 50, 60,$ and 70 m/s, respectively
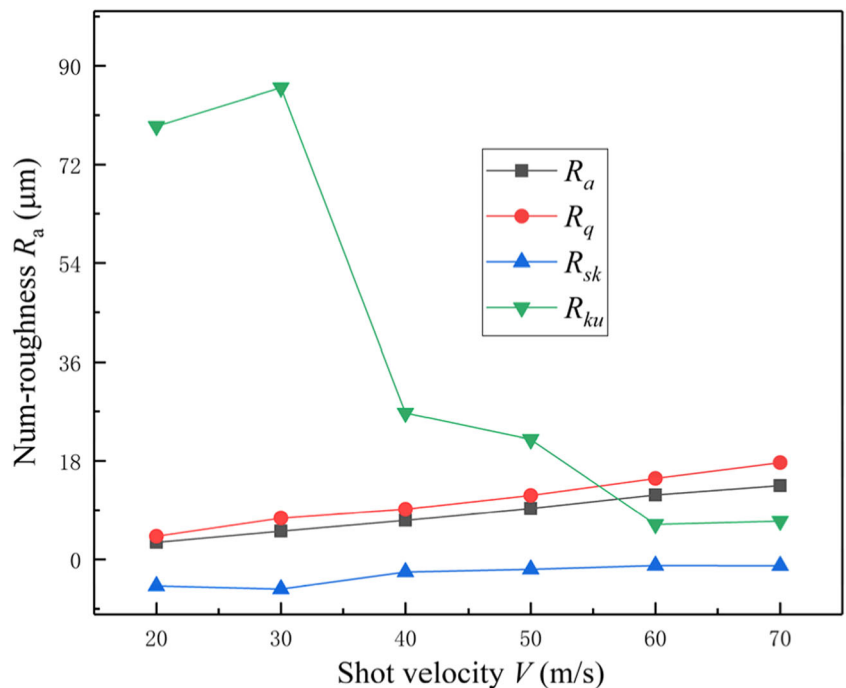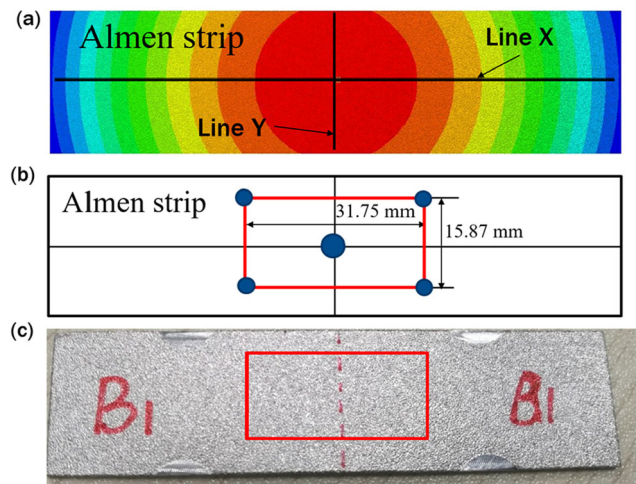
Fig. 16 Arc height by two method. **a** Deformation of the strip by direct simulation. **b** Measuring method by the Almen gauge. **c** Deformation of the strip after shot peening

simulated with a large of shots instead of elasticity theory as shown in Fig. 16, where shot velocity $V$ is equal to 44 m/s, 50 m/s, 57 m/s, corresponding to air pressure $P$ is equal to 2.0, 2.5, 3.0 bar. Figure 17 shows that these arc heights of experimental methods and numerical methods are in close agreement, and the equivalent shot velocity corresponding to the air pressure is accurate.

### 4.2.2 Residual stress verification

Through successive impacts on the strip, which is fixed into place using the Almen holder, the energy stored in the vast shots transfers into the peened material and induces a compressive residual stress field near the surface called induced stress. After removal of the Almen holder, and due to the
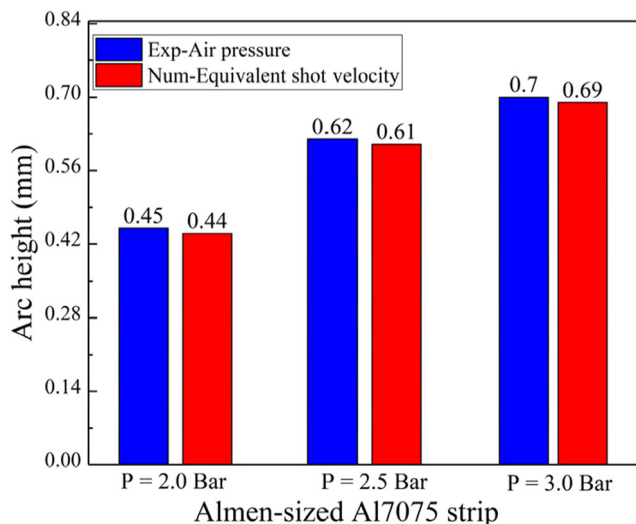
change in the boundary conditions, the nonequilibrated-induced stress forces the Almen strip to bend toward the impacted direction to form the arc height. The stress state of the strip is converted from induced stress near the surface to equilibrium residual stress of the whole strip thickness direction. The induced stress is difficult to be measured by the experimental method, but the induced stress and residual stress can be easily obtained by the simulation method proposed by the paper. In order to further verify the reliability and correctness of the new method, the residual stress obtained by simulation is compared to the experimental ones by using X-ray diffraction method, as illustrated in Fig. 18a. Compared with the result, the distribution trend of residual stress measured by the experiment is consistent as shown in Fig. 18b.

### 4.2.3 Coverage verification

Gangaraj et al. [22] questioned previous methods of calculating coverage and proposed a new method to obtain the coverage. Figure 19a demonstrate the displacement perpendicular to the surface cross-section along with PEEQ around the impingement center. When shot velocity $V$ is equal to 30 m/s, the indentation radiuses $r$ formed after a single impingement were 0.115 mm. The amounts of PEEQ at the boundary of indentation were 0.05. In this paper, we use the method proposed by Gangaraj et al. [22] to calculate the coverage by formula 16 and 17, which is closer to the experimental results as shown Fig.19b.

$$C\% = 100\left(1-e^{-A_r}\right) \tag{16}$$

$$A_r = N\frac{\pi r^2}{2.25} \tag{17}$$

### 4.3 Comparison of the new method with the semi-experiential formula

In order to compare with shot, velocity was estimated by the semi-experiential formula introduced by Klemenz et al. [6], which is shown below in Eq. (18).

$$V = \frac{163.5 \times P}{1.53 \times M + 10 \times P} + \frac{295 \times P}{0.598 \times d + 10 \times P}$$
$$+ 48.3 \times P \tag{18}$$

where $V$, $P$, $M$, and $d$ represent velocity of the shot ball(m/s), the air pressure (MPa), the mass flow (kg/min), and the diameter of shot balls (mm), respectively, for the given shot type (S230 steel shots with the diameter of 0.58 mm) and the value of mass flow of 5.0 kg/min. As it can be seen, the equivalent shot velocity measured by the new method introduced in this paper is always larger than that calculated by Klemenz et al.



Fig. 17 Arc height comparison of two methods
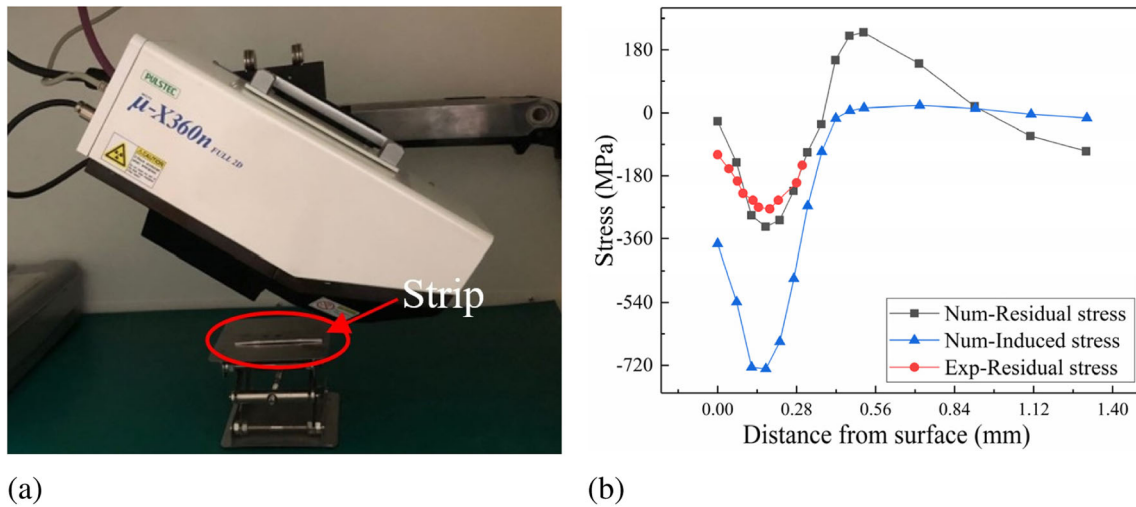
**Fig. 18** Residual stress. **a** X-ray diffraction method. **b** The new method is verified by residual stress, *V* is equal to 44 m, corresponding to *P* is equal to 2.0 bar

[6], as shown in Fig. 20. With the increase of air pressure (the air pressure *P* is greater than 1.0 bar), the velocity difference between the two methods is not larger, and the similar curve profile can be promising. However, they drift away as the air pressure increases. This can be explained by the fact that the formula is not applicable to all shot peening machines.

## 4.4 Comparison date and time-consuming of two method

In order to reflect the advantages of the model proposed in this paper, we compared the DEM-FEM model with the FEM model in terms of node, element, and time-consuming as shown in Fig. 21. It can be seen from Table 3 that

(1) The number of nodes and elements in the DEM-FEM model is approximately one-third of the FEM model. The main reason is that the PD3D element in the DEM-FEM model is a single-node rigid element (no mesh is need).

(2) The ODB file of the DEM-FEM model is 796,096 KB, and the ODB file of the FEM model is 5,292,331 KB. The main reason for the reduced size of the ODB file is that no element output is available for PD3D elements and the volume average output for stress, strain, and other similar continuum element output is not available for DEM analysis.

(3) The execution time of the FEM model simulation is approximately 6 h, and the time-consuming of the DEM-FEM model simulation is approximately 2 h. The
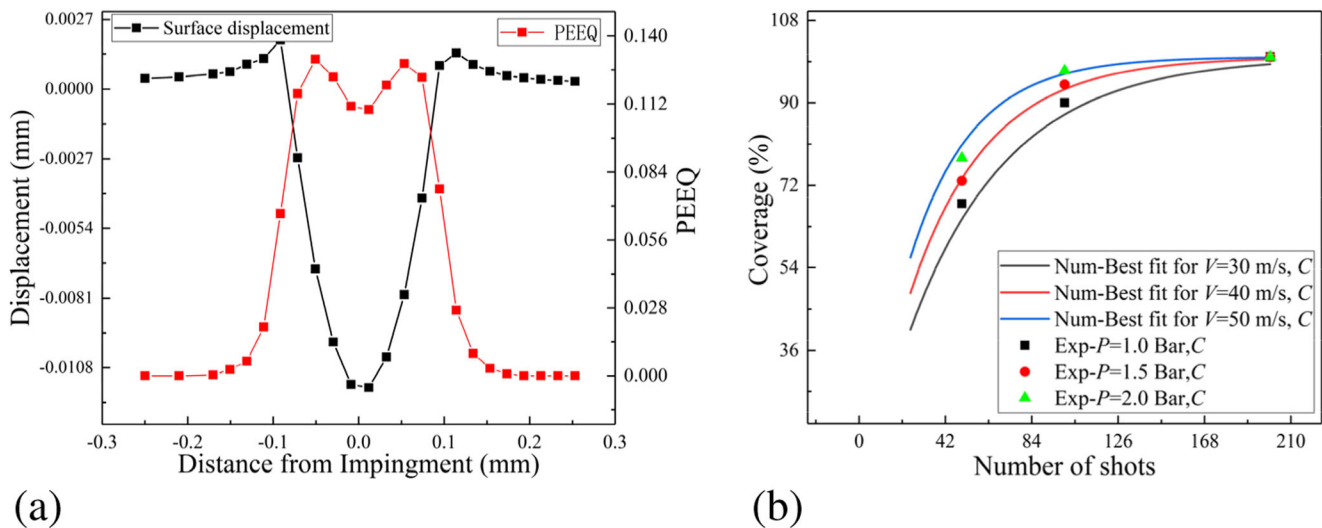


**Fig. 19** Coverage verification. **a** Indentation profile and plastic equivalent strain for single shot. **b** Experimental coverage and simulation coverage
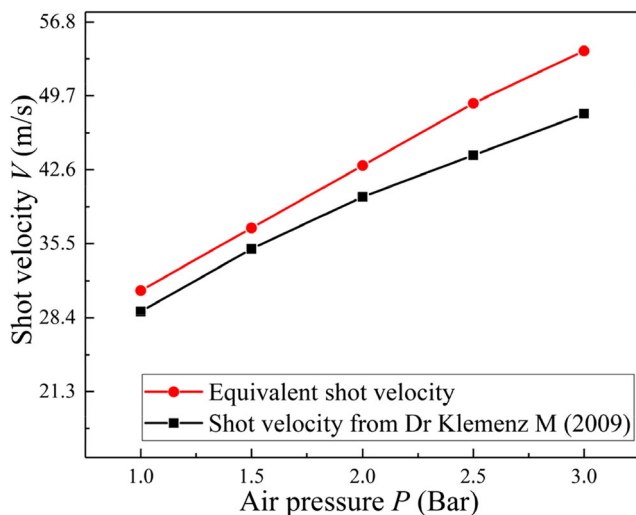
**Fig. 20** Relationship between shot velocity and air pressure obtained by the two methods

**Table 3** Compared with between FEM model and DEM-FEM model about data and time-consuming

|  | Node (No.) | Element (No.) | ODB file (KB) | Time (hour) |
|---|---|---|---|---|
| FEM model | 1,065,960 | 705,232 | 5,292,331 | 6.0 |
| DEM-FEM model | 297,160 | 282,282 | 796,096 | 2.0 |

analyses are both run on a single computer with an Intel Xeon E5-2640 processor with 15 MB Smartcache and 64 GB of memory running Windows 10. The solving efficiency of DEM-FEM method is three times that of FEM method.

## 5 Conclusions

This paper provides an effective and fast method to determine the equivalent shot velocity used in shot peening simulation corresponding to the air pressure in the actual shot peening process. The 3D DEM-FEM model proposed in this paper takes into account the collision between the shots and has more advantages. Then, this paper introduces a new method to calculate the number of shots used in simulation, considering test process parameters such as the mass flow rate, nozzle movement speed, and nozzle-workpiece distance. At last, the simple linear relationship between equivalent shot velocity used in simulation and air pressure in the actual shot peening process is established by the intermediate surface roughness. The method proposed in this paper is especially suitable for the operation, simulation prediction, and optimization of shot peening process for aerospace and automotive industry.

In this paper, the main findings are as follows:

1: Collisions between shots are considered in DEM-FEM model. This model is closer to the actual shot peening situation and have more advantages.

2: This paper introduces a new method to calculate the number of shots used in simulation, considering test process parameters such as the mass flow rate, nozzle movement speed, and nozzle-workpiece distance.

3: For the given shot type, mass flow, and other process parameters, the equivalent shot velocity for simulation

**Fig. 21** DEM-FEM and FEM
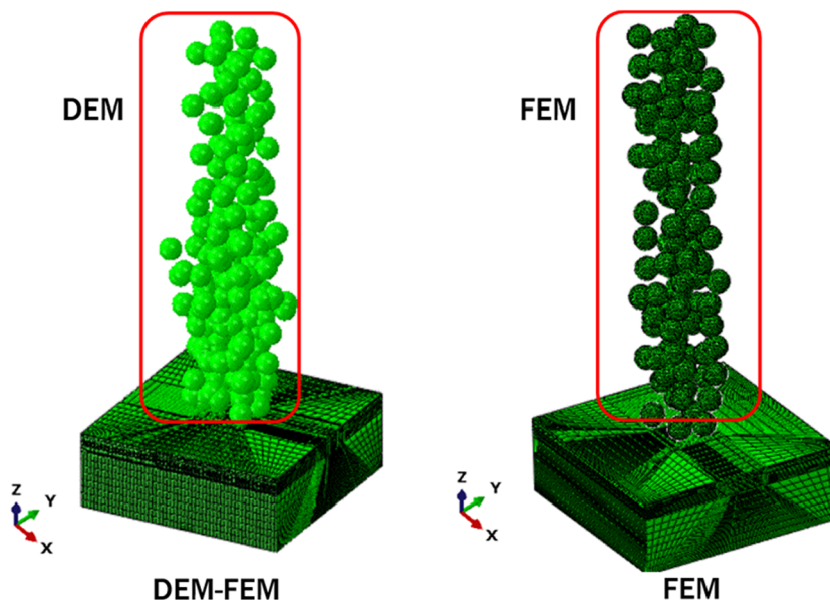
corresponding to the air pressure in the actual shot peening process can be quickly determined by this new method. The equivalent shot velocity may not be the real shot velocity, but the shot peening effect is maintained in terms of surface roughness, residual stress, arc height deformation, and coverage in the simulation analysis. The new method has the advantage of simple formula form, single variable, specific to the peening machine (the air pressure $P$ is greater than 0.1 MPa).

# References

1. Miao HY, Demers D, Larose S, Perron C, Lévesque M (2010) Experimental study of shot peening and stress peen forming. J Mater Process Technol 210(15):2089–2102

2. Hu Y, Zhang W, Jiang W, Cao L, Shen Y, Li H, Guan Z, Tao J, Xu J (2016) Effects of exposure time and intensity on the shot peen forming characteristics of Ti/CFRP laminates. Compos A: Appl Sci Manuf 91:96–104

3. Jebahi M, Gakwaya A, Lévesque J, Mechri O, Ba K (2016) Robust methodology to simulate real shot peening process using discrete-continuum coupling method. Int J Mech Sci 107:21–33

4. Miao HY, Larose S, Perron C, Lévesque M (2010) An analytical approach to relate shot peening parameters to Almen intensity. Surf Coat Technol 205(7):2055–2066

5. Zhang XJ, Wang T, Wang JB, Liu C (2017) Analytical modeling of shot peen forming process using cross-sectional linear indentation coverage method. Int J Mech Sci 133:838–845

6. Klemenz M, Schulze V, Rohr L, Löhe D (2009) Application of the FEM for the prediction of the surface layer characteristics after shot peening. J Mater Process Technol 209:4093–4102

7. Bill B, Kevin Y (2005) Particle velocity sensor for improving shot peening process control. Technological Aspects 385:2005114

8. Mylonas GI, Labeas G (2011) Numerical modelling of shot peening process and corresponding products: residual stress, surface roughness and cold work prediction. Surf Coat Technol 205(19):4480–4494

9. Gariépy A, Miao HY, Lévesque M (2017) Simulation of the shot peening process with variable shot diameters and impacting velocities. Adv Eng Softw 114:121–133

10. Tu F, Delbergue D, Miao H, Klotz T, Brochu M, Bocher P, Levesque M (2017) A sequential DEM-FEM coupling method for shot peening simulation. Surf Coat Technol 319:200–212

11. Hong T, Ooi JY, Shaw B (2008) A numerical simulation to relate the shot peening parameters to the induced residual stresses. Eng Fail Anal 15(8):1097–1110

12. Nordin E, Alfredsson B (2016) Measuring shot peening media velocity by indent size comparison. J Mater Process Technol 235:143–148

13. Liu ZY, Guo YB, Huang CZ (2016) Kinematic modeling and deformation mechanics in shot peening of functional ceramics. Procedia Manuf 5:508–520

14. Miao H, Mendez Romero JA, Forgues S, Lévesque M (2020) Experimental and numerical study of pneumatic needle peening effects on aluminium alloy 2024-T3. J Mater Process Technol 275:116370

15. Bagherifard S, Ghelichi R, Guagliano M (2012) Numerical and experimental analysis of surface roughness generated by shot peening. Appl Surf Sci 258(18):6831–6840

16. Liu YG, Li MQ, Liu HJ (2017) Nanostructure and surface roughness in the processed surface layer of Ti-6Al-4V via shot peening. Mater Charact 123:83–90

17. Taro M, Chaise T, Nélias D (2015) A methodology to predict the roughness of shot peened surfaces. J Mater Process Technol 217:65–76

18. Lin Q, Liu H, Zhu C, Parker R (2019) Investigation on the effect of shot peening coverage on the surface integrity. Appl Surf Sci 489:66–72

19. Chen H, Wang S, Lu S, QIao Y, Wang X, Fan N, Guo P, Niu J (2018) Simulation and experimental validation of residual stress and surface roughness of high manganese steel after shot peening. In: Proceedings of the 4th CIRP Conference on Surface Integrity, pp 227–231

20. Kumar RK, SampathKumaran P, Seetharamu S, Kumar SA, Pramod T (2019) Investigation of shot peeing effect on titanium alloy affecting surface residual stress and roughness for aerospace. In: Proceedings of the 2nd International Conference on Structural Integrity and Exhibition 2018, pp 134–141

21. Wang X, Wang Z, Wu G, Gan J, Yang Y, Huang H, He J, Zhong H (2019) Combining the finite element method and response surface methodology for optimization of shot peening parameters. Int J Fatigue 129:105231

22. Gangaraj SMH, Guagliano M, Farrahi GH (2014) An approach to relate shot peening finite element simulation to the actual coverage. Surf Coat Technol 243:39–45

23. Han K, Owen DRJ, Peric D (2002) Combined finite/discrete element and explicit/implicit simulations of peen forming process. Eng Comput 19(1):92–118

24. Huang H, Wang Z, Gan J, Yang Y, Wang X, He J, Gan X (2019) The study of universality of a method for predicting surface nanocrystallization after high energy shot peening based on finite element analysis. Surf Coat Technol 358:617–627

25. Marini M, Fontanari V, Bandini M, Benedetti M (2017) Surface layer modifications of micro-shot-peened Al-7075-T651: experiments and stochastic numerical simulations. Surf Coat Technol 321:265–278

26. Xf S, Qx X, Cheng X, Lin L (2012) Residual stress field induced by shot peening based on random-shots for 7075 aluminum alloy. Trans Nonferrous Metals Soc China 22:s261–s267

27. Han K, Peric D, Crook AJL, Owen DRJ (2000) A combined finite/discrete element simulation of shot peening processes - part I: studies on 2D interaction laws. Eng Comput 17(5):593–619

28. Murugaratnam K, Utili S, Petrinic N (2015) A combined DEM–FEM numerical method for shot peening parameter optimisation. Adv Eng Softw 79:13–26

29. Gariépy A, Larose S, Perron C, Lévesque M (2011) Shot peening and peen forming finite element modelling – towards a quantitative method. Int J Solids Struct 48(20):2859–2877

30. Miao HY, Larose S, Perron C, Lévesque M (2009) On the potential applications of a 3D random finite element model for the simulation of shot peening. Adv Eng Softw 40(10):1023–1038

31. Wu J, Liu H, Wei P, Lin Q, Zhou S (2020) Effect of shot peening coverage on residual stress and surface roughness of 18CrNiMo7-6 steel. Int J Mech Sci 183:105785